


ARTICLE OPEN ACCESS

Engineering Affibody Binders to Death Receptor 5 and Tumor Necrosis Factor Receptor 1 With Improved Stability

Gregory H. Nielsen¹ | Jonathan N. Sachs² | Benjamin J. Hackel^{1,2} ¹Department of Chemical Engineering and Materials Science, University of Minnesota Twin Cities, Minneapolis, Minnesota, USA | ²Department of Biomedical Engineering, University of Minnesota Twin Cities, Minneapolis, Minnesota, USA**Correspondence:** Benjamin J. Hackel (hackel@umn.edu)**Received:** 9 November 2024 | **Revised:** 4 February 2025 | **Accepted:** 9 February 2025**Funding:** This research was supported by the National Institutes of Health (R01 EB028274 and R01 GM146372).**Keywords:** affibody | death receptor 5 | developability | evolution | tumor necrosis factor receptor

ABSTRACT

Protein developability is an important, yet often overlooked, aspect of protein discovery campaigns that is a key driver of utility. Recent advances have improved developability screening capacity, making it an increasingly viable option in early-stage discovery. Here, we engineered one component of developability, stability, of two affibody proteins—one that targets death receptor 5 and another that targets tumor necrosis factor receptor 1—previously evolved to bind receptor and non-competitively inhibit signaling via conformational modulation. Starting from an error-prone PCR library of each affibody, variants were screened via yeast surface display binder selections, including depletion of non-specific binders, followed by developability assessment using the on-yeast protease and yeast display level assays. Multiplex deep sequencing identified variants for further evaluation. Purified variants exhibited elevated stability—8°C to 14°C increase in $T_{m,app}$ —with maintained 1–2 nM affinity for the TNFR1 affibody and 30-fold improvement in the DR5 affibody affinity to 0.8 nM.

1 | Introduction

Effective protein therapeutics, diagnostics, and reagents require strong performance of their primary function (i.e., binding to a target) as well as biophysical robustness to render it viable in its desired application: to be efficiently produced; stable to temperature, protease, and complex chemical environments; soluble; and lacking in off-target interactions. These properties, termed developability (Jain et al. 2023, 2017; Fernández-Quintero et al. 2023), are often addressed separately from discovery of primary function. Satisfying both function and developability requirements simultaneously is a large hurdle required to bring a newly designed therapeutic to clinical testing (Tokuriki et al. 2008; Tokuriki and Tawfik 2009). Thus, it is important to utilize reliable and efficient screening methods to

both lower research and development costs and enable life-changing treatments to reach patients sooner (Jain et al. 2017). Recent advances have enabled library-scale experimental evaluation (Shusta et al. 1999; Rocklin et al. 2017; Golinski et al. 2021; Kelly et al. 2017) or computational design of developability (Fernández-Quintero et al. 2023; Wolf Pérez et al. 2019; Golinski et al. 2023; Chen et al. 2023). Herein, we leverage two library-scale developability screens—(1) protease resistance quantified by flow cytometric stratification of yeast-displayed protein variants on the basis of intact protein (Rocklin et al. 2017; Golinski et al. 2021; Klesmith et al. 2019; Ritter and Hackel 2019); and (2) yeast soluble expression and display under thermal stress (Shusta et al. 1999; Hackel et al. 2010; Shusta et al. 2000; Jones et al. 2011)—partnered with yeast-display binder screening methods (Yeung and Wittrup 2002;

This is an open access article under the terms of the [Creative Commons Attribution-NonCommercial-NoDerivs](https://creativecommons.org/licenses/by-nc-nd/4.0/) License, which permits use and distribution in any medium, provided the original work is properly cited, the use is non-commercial and no modifications or adaptations are made.

© 2025 The Author(s). *Biotechnology and Bioengineering* published by Wiley Periodicals LLC.

Van Antwerp and Wittrup 2000; Chen et al. 2013) to identify protein variants with elevated stability and maintained or improved binding.

The two proteins under study are derived from the affibody domain (Nord et al. 1997; Löfblom et al. 2010), a 58 amino acid three-helix bundle ligand scaffold that has been engineered to bind various targets and applied to therapeutics and diagnostics. The first ligand targets death receptor 5 (DR5), which is a compelling clinical target for treatment of non-alcoholic fatty liver disease (Hirsova et al. 2016; Hirsova and Gores 2015; Cazanave et al. 2011). Past approaches to DR5 inhibition have been accomplished by globally blocking the tumor necrosis factor family of ligands, however these approaches generally have substantial side effects due to their broader impact on the immune system (Wolfe and Michaud 2004; Shakoor et al. 2002). We recently discovered an affibody that allosterically modulates DR5, without competing with the native ligand TRAIL, to inhibit apoptosis in an in vitro model of fatty acid liver disease (Vunnam et al. 2020). The affibody's developability has not yet been characterized, and maturation of high-nM affinity may be beneficial. The second molecule of interest in the current study is an affibody engineered to bind tumor necrosis factor receptor 1 (TNFR1) and non-competitively inhibit TNF signaling with an IC_{50} of 0.23 nM (Vunnam et al. 2023). Multiple FDA-approved therapies for inflammatory and autoimmune diseases inhibit TNF, however they have suffered from side effects caused by ligand inhibition that impacts the entire TNF family (Cortese et al. 2021; Probert 2015; Fischer et al. 2020). The evolved affibody molecule was shown to specifically inhibit TNFR1 while not blocking TNFR2, which should yield fewer side effects.

The focus of this work was to improve upon the developability profiles, particularly stability, of these two affibody molecules while retaining or improving target binding affinity. Yeast display sorts were used to first screen variants of each library for binding while depleting non-specific binders, then screen binders from each library using the on-yeast protease assay (Rocklin et al. 2017; Golinski et al. 2021; Klesmith et al. 2019; Ritter and Hackel 2019) and yeast display level assay (Shusta et al. 1999; Hackel et al. 2010). Multiplex deep sequencing was used to assign developability scores to variants, informing the selection of a subset to characterize. Two TNFR1 variants and one DR5 variant were selected and shown to have enhanced thermal stability and similar or better binding than the parental affibodies, which renders them as compelling lead molecules for further therapeutic development.

2 | Results

2.1 | Library Creation

DNA encoding the parental DR5- and TNFR1-binding affibodies from past works (ABY_{DR5-P}, Vunnam et al. 2020, and ABY_{TNFR1-P}, Vunnam et al. 2023) was mutated via error-prone PCR using nucleotide analogs 8-oxo-dGTP and dPTP (Zaccolo et al. 1996). By varying cycle numbers and analog concentrations, as previously modeled (Hackel 2009), four sets of mutated DNA were generated with different error rates and pooled for each target. This allowed for a wider distribution of both

conservatively low mutation rates as well as higher mutational load that may have a lower frequency of success but a higher potential benefit for the best variants (Drummond et al. 2005). The pooled libraries were transformed into a yeast surface display system as genetic fusions to Aga2p with a flexible peptide linker (Aga2p-linker-affibody) resulting in 56 and 80 million variants of ABY_{DR5-P} and ABY_{TNFR1-P}, respectively. Multiplex deep sequencing revealed the desired broad distribution of amino acid mutations (Supporting Information S1: Figure S1).

2.2 | Library Selections

The libraries were sorted for binding and developability. As the libraries were created from parental molecules that bind the desired target, an aggressive binder screening approach was implemented. First, non-specific binders were depleted by removing variants that bound to multivalently-presented binding immunoglobulin protein, a process that has been previously validated (Kelly et al. 2017; Nielsen et al. 2024). The remaining variants were then screened via monovalent magnetic activated cell sorting (MACS): affibody-displaying yeast were incubated with detergent-solubilized lysate of biotinylated DR5- or TNFR1-expressing HEK293 cells; after washing, target-bound yeast were collected via pull-down with avidin-coated magnetic beads. The binder pool obtained from one round of monovalent MACS was then screened via one round of fluorescent activated cell sorting (FACS) using detergent-solubilized cell lysate of HEK293 cells overexpressing GFP fusions of DR5 or TNFR1. Incubation with 2 nM (DR5, Figure 1B) or 5 nM (TNFR1, Figure 1C) lysate yielded distinct binding signal relative to lysate-free controls (Figure 1D,E) for numerous ligand variants. Binding variants were collected from the best 0.2% of binders and the next 2% of binders.

The enriched binder populations were next sorted for developability via a pair of yeast surface display selections. Yeast-displayed binder populations were sorted (one round each) for stability by incubating induced yeast at 37°C with proteinase K and selecting variants with the highest fraction of full-length affibodies, identified as the ratio of C-terminal cMyc epitope relative to N-terminal HA epitope. A broad range of stability was observed for both the strongest and 2nd-tier binders to DR5 (Figure 2B) and TNFR1 (Figure 2C), with numerous binders exhibiting strong stability. To assess reliability, the TNFR1 protease sort of strong binders, along with deep sequencing, was performed in duplicate, and assay scores from both trials correlated well (Pearson ρ = 0.70, Supporting Information S1: Figure S2).

The enriched binder populations were also sorted (one round each) for expression under thermal stress by inducing yeast at an elevated temperature (37°C). This assay has previously exhibited correlation with soluble secretion efficiency and thermal stability for single-chain antibody fragments (Shusta et al. 1999), enhanced expression and stability of hepatocyte growth factors (Jones et al. 2011) and thermal stability for fibronectin domains (Hackel et al. 2010) and single-chain T cell receptors (Shusta et al. 2000). Yeast were sorted based on the number of affibody molecules expressed and displayed per cell, measured via a C-terminal cMyc epitope (Figure 2D–F). In both

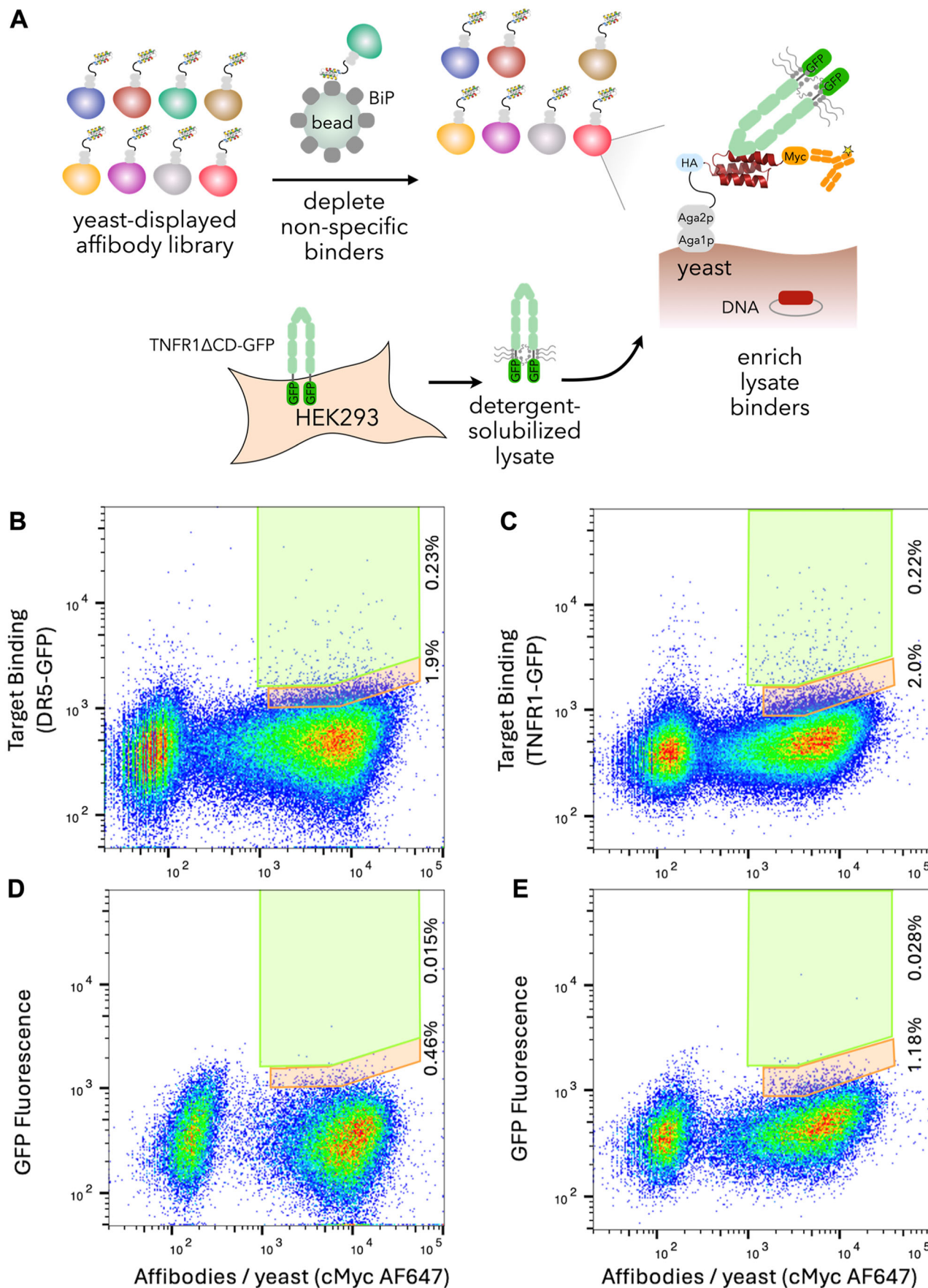


FIGURE 1 | Legend on next page.

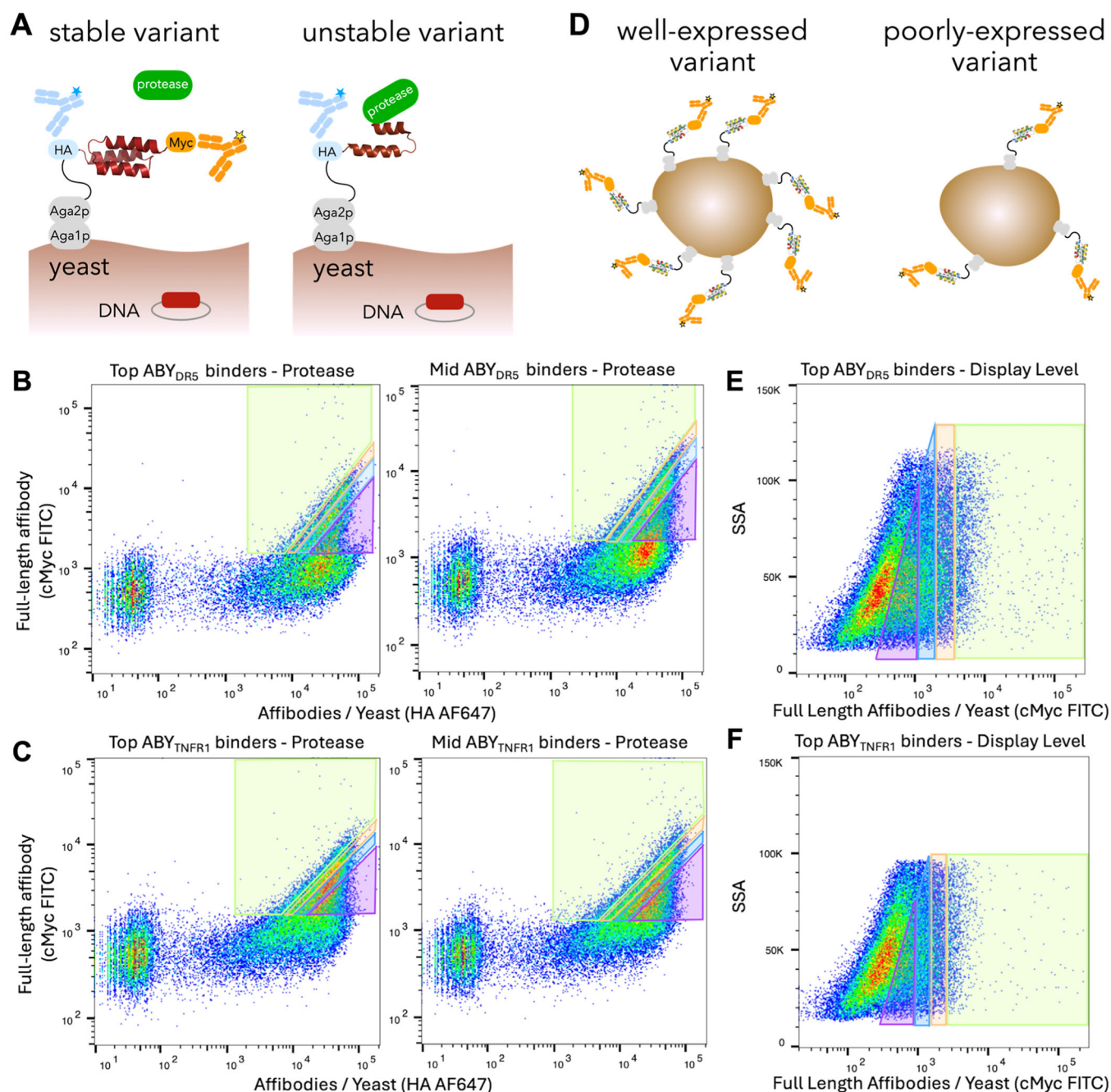


FIGURE 2 | Developability selections. Yeast displaying populations enriched for binding via flow cytometry were evaluated and sorted for protease resistance at 37°C (A–C) and expression under thermal stress (D–F). The input to each of these screens was the binder population sorted via FACS (as shown in Figure 1). Both top and mid gates were sorted with the on-yeast protease sort whereas only the top binder gate was sorted with the display level sort. In all cases, gates drawn contain the top 10% of cMyc⁺ variants, next 20%, next 30%, then remaining 40%.

FIGURE 1 | Binding selections. (A) Schematic of selection strategy. (B–E) Yeast displaying ligand populations depleted for non-specific binders and enriched for binders to DR5 (B) or TNFR1 (C) were labeled with detergent-solubilized cell lysate containing 2 nM DR5-GFP (B) or 5 nM TNFR1-GFP (C) as well as co-labeling of full-length affibodies via anti-cMyc-AF647 conjugate. The top 0.2% and next 2% of binders were collected from each library. Gates were drawn with a GFP:cMyc diagonal to normalize binding relative to affibodies displayed per cell, except at low expression to avoid collecting in the GFP background regime. Lysate-free controls for DR5 (D) and TNFR1 (E) populations provide a comparison for yeast cellular autofluorescence. Non-binding affibody variants within the analyzed population provide a comparative control demonstrating the lack of non-specific binding of GFP fusions.

cases, four gates were collected with the top 10% of developable (cMyc⁺) variants, next 20%, next 30%, and remaining 40%. Variants were scored as a weighted average location of their appearance from deep sequencing data.

2.3 | Variant Selection and Testing

Variants were selected for characterization based on multiplex deep sequencing enrichments and assay scores. Enrichment from the error-prone PCR library to the FACS sorted binder library was used to rank variants by binding strength. Developability was assessed via the on-yeast protease and yeast display level assay scores. Variants yielding above average scores in all three metrics were selected (Supporting Information S1: Figures S3 and S4), yielding 10 DR5 and 8 TNFR1 variants (Supporting Information S1: Tables S1 and S2).

The 18 selected variants and the parentals were produced in an *Escherichia coli* expression system. Production purity and titer were assessed via SDS-PAGE, and variants with low titer or low purity were not further pursued (Supporting Information S1: Tables S1, S2 and Figures S3, S4). Notably, the lowest scoring yeast display level variants for each library, ABY_{DR5-2} and ABY_{TNFR1-2}, both expressed poorly (Supporting Information S1: Figure S5). Yet, overall correlation between yeast display score and soluble expression yield was moderate ($\rho = 0.26$); for example, ABY_{TNFR1-4} was tied for the highest yeast display level score of all TNFR1 variants, yet did not express well in *E. coli*, so the predictive capacity of this assay should be analyzed further for affibodies.

Four variants for each target, exhibiting at least moderate titer and purity, were selected for binding evaluation. HEK293 cells overexpressing either DR5 or TNFR1 were incubated with 2 or 20 nM of each protein variant, followed by an anti-His₆ fluorescent antibody. Binding affinity was assessed via flow cytometry. Three variants with the highest binding signal—ABY_{DR5-3}, ABY_{TNFR1-5}, and ABY_{TNFR1-7} (Supporting Information S1: Figures S6 and S7)—were chosen for deeper analysis. Amino acid sequence and multiplex deep sequencing data for each of these variants as well as the two parentals is found in Table 1.

Affinity titrations were performed for each variant, in the purified affibody format, using HEK293 cells overexpressing DR5 or TNFR1 (Figure 3). ABY_{DR5-3} binds 30-fold more strongly than the parental ABY_{DR5-P} ($K_d = 0.79$ nM, 95% confidence interval: 0.28–1.7 nM, as compared to 24 nM [6.1–120 nM] for parental; Figure 3B). The three TNFR1 variants exhibit binding affinity closely aligned with ABY_{TNFR1} parental affinity (Figure 3C). The stronger binding improvement of ABY_{DR5-3} aligns with higher relative enrichment in the library-scale binding sorts (Table 1). Also, two of the mutations in ABY_{DR5-3} (I16V and I31M) are within the engineered paratope region whereas all mutations within ABY_{TNFR1-5} and ABY_{TNFR1-7} are separate from the engineered paratope, although proximal (Figure 4).

Circular dichroism was used to assess thermal stability for the five analyzed variants. The apparent midpoint of thermal denaturation ($T_{m,app}$) was calculated for each variant by fitting a standard two-state unfolding curve to the ellipticity data (Figure 5). The two TNFR1-targeted variants had substantially

TABLE 1 | Amino acid sequences and library-scale assay scores of variants selected for full characterization via affinity titration and circular dichroism. Mutations away from parental are highlighted in red.

Site number	1	2	3	4	5	6	7	8	9	10	11	12	13	14	15	16	17	18	19	20	21	22	23	24	25	26	27	28	29	30	31	32	33	34	35	36	37	38	39	40	41	42	43	44	45	46	47	48	49	50	51	52	53	54	55	56	57	58	FACS Enrich	Protease score	Display score																																																																																																																																																																																																																																																																																																																																																																																																																																																																																																																																																																																																																																																																																																																																																																																																																																																																																																																																																																																																																																																																																																																																																																		
ABY _{DR5-P}	A	E	A	K	Y	A	K	E	D	Y	L	A	V	V	E	I	V	G	L	P	N	L	T	L	G	Q	T	L	A	F	I	F	A	L	G	D	D	P	S	Q	S	E	L	S	E	A	K	K	L	N	D	S	Q	A	P	K	0.18	0.39	0.66																																																																																																																																																																																																																																																																																																																																																																																																																																																																																																																																																																																																																																																																																																																																																																																																																																																																																																																																																																																																																																																																																																																																																																				
ABY _{DR5-3}	A	E	A	K	Y	A	K	E	D	Y	L	A	V	V	E	I	V	G	L	P	N	L	T	L	G	Q	T	L	A	F	I	F	A	L	G	D	D	P	S	Q	S	E	L	S	E	A	K	K	L	N	D	S	Q	A	P	R	390	0.48	0.65																																																																																																																																																																																																																																																																																																																																																																																																																																																																																																																																																																																																																																																																																																																																																																																																																																																																																																																																																																																																																																																																																																																																																																				

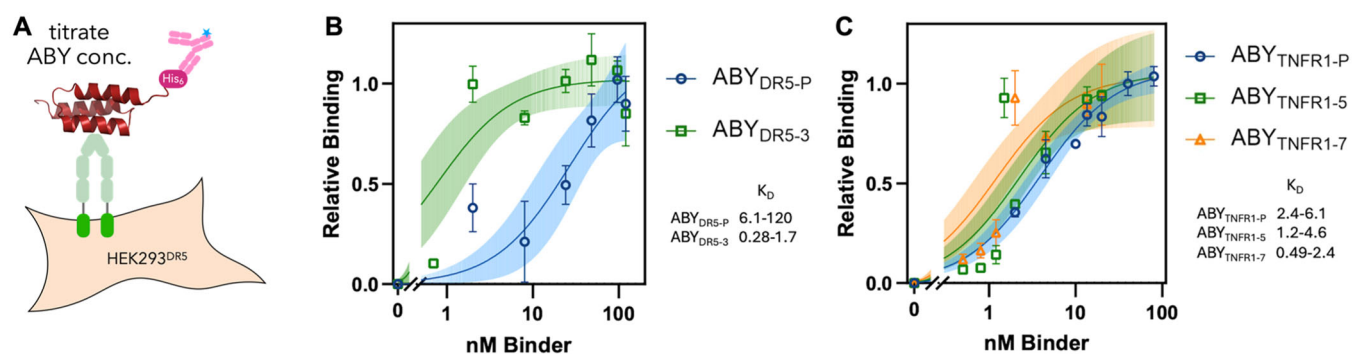


FIGURE 3 | Affinity titrations. HEK293 cells overexpressing DR5-GFP (B) or TNFR1-GFP (C) were incubated with varying concentrations of purified affibody variants followed by anti-His₆-APC (A). Binding was detected via flow cytometry. K_d was computed by minimization of the sum of squared errors for a 1:1 binding. Error bars indicate standard error of the mean for at least four samples per data point (duplicate samples each day for at least 2 days). The colored band around the fit line indicates the 95% confidence interval of the best fit line. The 95% confidence interval for each K_D is listed under the legend for each figure. Individual affinity titration curves can be found in the supplement (Supporting Information S1: Figure S8).

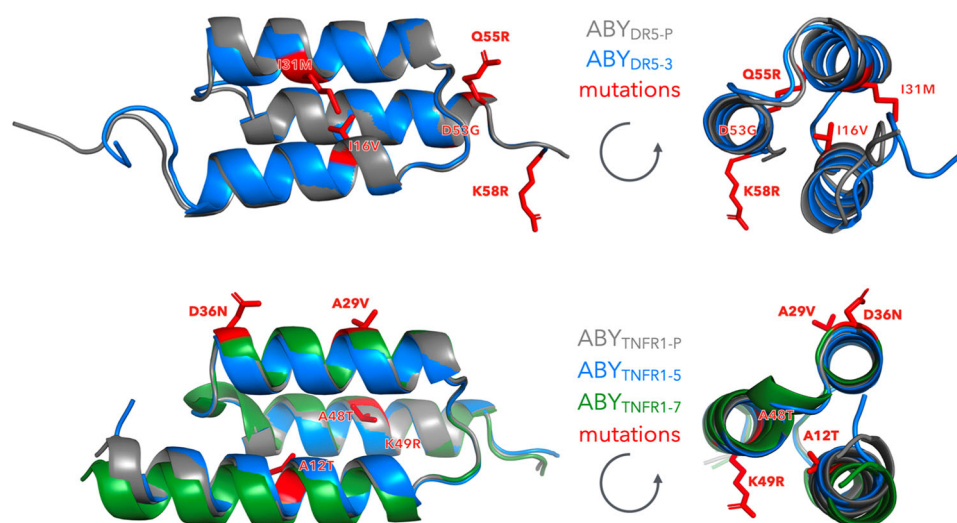


FIGURE 4 | Structural analysis. Structures of the affibody variants were predicted with AlphaFold3 (Abramson et al. 2024) and aligned within PyMol (DeLano 2002). Mutations in ABY_{DR5-3} and ABY_{TNFR1-7} relative to parentals (gray) are depicted in red sticks. The region originally engineered to discover the parental binders is on the surface of the first two helices, which are at the “front” of the frontal perspectives (left images) and on the right of the coronal perspectives (right images).

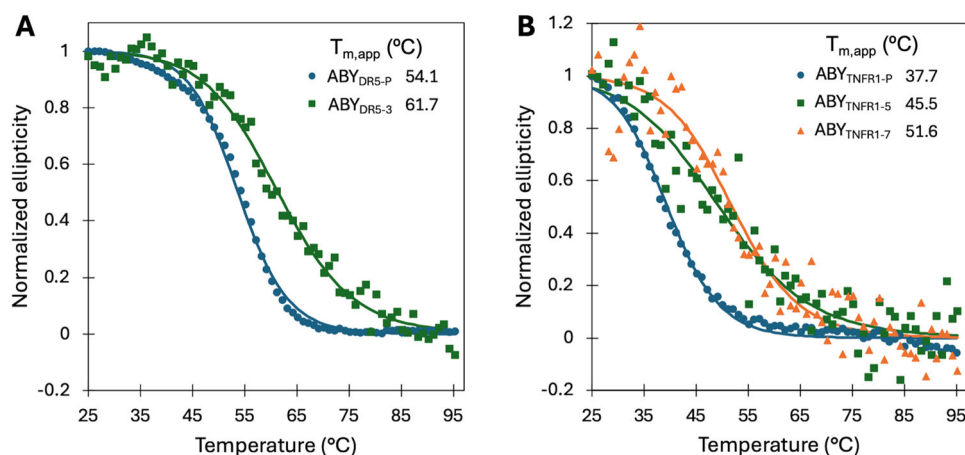


FIGURE 5 | Stability analysis. Purified DR5-binding (A) and TNFR1-binding (B) affibody variants were evaluated by circular dichroism spectroscopy. Molar ellipticity at 216 nm was measured as temperature was increased from 25°C to 95°C (at a rate of 3°C/min). $T_{m,app}$ was computed using a two-state unfolding model (shown as solid line). Individual thermal denaturation curves can be found in the supplement (Supporting Information S1: Figure S9).

higher $T_{m,app}$'s (46°C and 52°C) relative to the parental $T_{m,app}$ of only 38°C (Figure 5B). For DR5 targeting, ABY_{DR5-P} had a higher starting $T_{m,app}$ of 54°C and was further stabilized as variant ABY_{DR5-3} to $T_{m,app} = 62°C$ (Figure 5A). The increased thermal stabilities of all three variants are consistent with higher scores in the library-scale protease resistance assay (Table 1). Structural analysis (Figure 4) suggests potential sources of stabilization. The ABY_{DR5-3} mutations include two hydrophobic mutations—one with full burial (I16V, 0% solvent accessible surface area [SASA]) and one with moderate burial (I31M, 33% SASA)—as well as three mutations at hydrophilic sites near the C-terminus. The $ABY_{TNFR1-7}$ mutations include two buried hydrophobic mutations (A12T [6% SASA] and A48T [7%]) as well as three surface mutations.

3 | Discussion

We used an efficient library-scale yeast display screening approach, entailing three assays, to further engineer known affibody binders to DR5 and TNFR1 for improved stability and maintained binding affinity. A broadly diverse mutant space was narrowed to variants that lacked non-specific binding to avidin and binding immunoglobulin protein and maintained binding to DR5 or TNFR1 in the form of detergent-solubilized cell lysate. Binding strength was then evaluated by enrichment in a stringent flow cytometric selection. Parallel developability sorts—entailing (1) resistance to protease K degradation as assessed via maintenance of terminal epitopes as well as (2) soluble expression at elevated temperature—enabled stratification of variants via multiplex deep sequencing analysis. Variants with strong performance across all three assays were identified and evaluated as purified proteins. The DR5-binding variant ABY_{DR5-3} exhibited an 8°C increase in $T_{m,app}$ and a 30-fold improvement in binding affinity to 0.8 nM. A pair of TNFR1 binders, $ABY_{TNFR1-5}$ and $ABY_{TNFR1-7}$, were found to increase $T_{m,app}$ 8°C and 14°C, respectively, with similar or slightly improved binding affinities. The stability engineering provides a step towards $T_{m,app}$ benchmark values; for example, 90% of FDA approved antibodies have a $T_{m,app} \geq 64°C$ (Jain et al. 2023). We thought it valuable to report the stability and binding improvements as they increase the likelihood of clinical relevance for these affibodies, though future work with these variants should include cellular assays to more deeply assess maintenance of their target specificity (e.g., to DR4 and TNFR2) and non-competitive inhibitory potency as outlined in past work (Vunnam et al. 2020, 2023).

The efficiency of stability maturation accomplished herein motivates deeper integration of library-scale developability evaluation early in the protein discovery pipeline. The yeast display modality of the protease resistance and display level developability assays enables efficient integration with binding affinity selections. Collective evaluation of performance in the three assays readily identified performant variants. Soluble expression exhibited only modest correlation with yeast display level at elevated temperature, yet display levels may provide guidance for other performance metrics, such as the stability predictiveness the assay has demonstrated for other proteins (Shusta et al. 1999; Hackel et al. 2010; Shusta et al. 2000; Jones et al. 2011). Maturation of other lead molecules, as well as

broader evaluation of additional candidate variants and additional metrics of clonal characterization, will provide insight on the relative utility of each assay.

4 | Materials and Methods

4.1 | Error-Prone PCR

Error-prone PCR was performed essentially as described previously (Hackel et al. 2008). Briefly, the entire affibody gene (174 nucleotides) was amplified using *Taq* DNA polymerase in conjunction with 8-oxo-dGTP and dPTP analogs at varying concentrations to induce copy errors. 1× ThermoPol buffer (New England Biolabs, NEB), 0.5 μM each of forward and reverse primers (Supporting Information S1: Table S3), 200 μM of each dNTP, either 20 or 200 μM of each analog, 2.5 units of *Taq* DNA polymerase (NEB), and 2 μL of plasmid miniprep template DNA was adjusted to 50 μL with ddH₂O. Amplifications were performed in 4 separate batches to achieve different error rates, informed by past work (Hackel 2009). The conditions were 20 μM analog for 10 or 15 cycles, or 200 μM analog for 5 or 10 cycles. PCR product from each of the 4 conditions was further amplified using the same primers and Phusion DNA polymerase (NEB) for 32 cycles to generate enough insert for electroporation and homologous recombination into yeast. Manufacturer's protocols were followed for the second amplification.

4.2 | Yeast Library Creation and Cell Maintenance

The pCT-80 yeast display vector (Lown et al. 2021) containing the N-terminal HA and C-terminal cMyc tags was digested with BamHI-HF and NheI-HF (NEB) according to manufacturer's protocols. Both digested vector and insert were ethanol precipitated by mixing with 10% v/v 3 M sodium acetate (pH 5.2). 3× volume of 100% ethanol was added and the mixture incubated at 4°C for 10 min. The mixture was then centrifuged for 20 min at 15,000g and 4°C, and the supernatant was removed. A total of 500 μL of 70% ethanol was added to the tube, and the mixture was briefly vortexed and centrifuged under the same conditions, removing the supernatant afterwards. A total of 500 μL of 100% ethanol was added, and the mixture was briefly vortexed and centrifuged with equivalent conditions. The supernatant was removed, and the pellet was left to air dry overnight. Each pellet was resuspended in buffer E (1 M sorbitol and 1 mM CaCl₂ in ddH₂O) before electroporation.

Competent EBY100 yeast was prepared as previously described (Woldring et al. 2015). A 100 mL EBY100 culture was grown to OD₆₀₀ 1.4, then harvested and pelleted (2250g for 3 min). The supernatant was removed, and cells were washed twice with 25 mL cold ddH₂O. Cells were washed once with cold buffer E and resuspended in 25 mL of 100 mM lithium acetate, 10 mM Tris (pH 7.5), 1 mM EDTA, 30% PEG 8000, and 10 mM dithiothreitol. Cells were incubated at 30°C and 250 RPM for 30 min. Cells were pelleted in a cold centrifuge, washed thrice with cold buffer E (all in a 4°C centrifuge), and resuspended in 300 μL buffer E.

Libraries were prepared for electroporation by combining 300 μL of electrocompetent EBY100 yeast, 6 μg digested vector, and ≥ 200 pmol of insert. Inserts from all 4 error-prone PCR conditions were pooled together as an equimolar mixture at this step. The mixture was added to a 2 mM cuvette and placed on ice for 5 min before electroporation. Following electroporation, cells were grown for 1.5 h in YPD medium (10.0 g/L yeast extract, 20.0 g/L peptone, 20.0 g/L dextrose) at 30°C, then switched to SD-CAA selective growth media (16.8 g/L sodium citrate dihydrate, 3.9 g/L citric acid, 20.0 g/L dextrose, 6.7 g/L yeast nitrogen base and 5.0 g/L casamino acids in dH_2O). Transformation efficiency was quantified by liquid culture growth rate at 30°C with shaking at 250 RPM in SD-CAA with an expected doubling time of 3.75 h.

To induce protein expression and display on yeast, culture exceeding an OD_{600} of 4 was centrifuged and media replaced with SG-CAA selective induction media (10.2 g/L sodium phosphate dibasic heptahydrate, 8.6 g/L sodium phosphate monobasic monohydrate, 19.0 g/L galactose, 1.0 g/L dextrose, 6.7 g/L yeast nitrogen base and 5.0 g/L casamino acids in dH_2O). Cells were induced by growing overnight at 30°C and 250 RPM. Induced yeast were stored at 4°C and used within 2 weeks.

4.3 | HEK293 Cell Maintenance and Transfection

Cultures of both standard HEK293 cells (ATCC CRL-3216) and those stably expressing DR5-GFP or TNFR1-GFP (Vunnam et al. 2020, 2023) (Supporting Information S1: Table S4) were maintained by growth in 75 cm^2 culture flasks at 37°C and 5% CO_2 in DMEM complete media containing 10% fetal bovine serum and 1% penicillin-streptomycin. For DR5 expressing HEK293 cells, 1% geneticin was also added. Cells were passaged at 50%–90% confluency by washing with phosphate-buffered saline (PBS, 4 mM phosphate, pH 7.4, 155 mM NaCl) and detaching with 2.5 mL of trypsin/EDTA for 3 min (all reagents from Gibco). A total of 5 mL of prewarmed DMEM complete media was added to inactivate the trypsin, and cells were spun down at 200g for 2 min after which the supernatant was removed. At this stage, cells were either added to a fresh flask to grow or further washed thrice with PBS. To create cell lysate for MACS or FACS, 100 μL of ice-cold cell lysis buffer (1% v/v Triton X-100 [ThermoFisher] and 2 mM EDTA in dH_2O with protease inhibitor cocktail) was added. Cells were incubated while rotating at 4°C for 20 min then centrifuged at 16,000g for 15 min to remove any insoluble cell debris. Supernatant was used as cell lysate.

HEK293 cells were transfected the day before each use via Fugene-6 transfection reagent (Promega). Fugene-6 reagent was removed from the fridge for 5 min before initiating the protocol. A total of 70.2 μL of Fugene-6 was added to a 1.5 mL tube with 1050 μL of Opti-MEM (Gibco), inverted three times and let sit for 5 min. A total of 23.4 μg of plasmid for expression of TNFR1-GFP was then added to the mixture to increase the total volume to 1170 μL . This mixture was allowed to incubate for 15 min, meanwhile the media of a flask of ~50% confluent HEK293 cells was replaced with 9 mL fresh, warm DMEM complete media. After the incubation, the entire 1170 μL mixture was added to the flask and cells were allowed to grow overnight.

4.4 | Carboxylic Acid Bead Preparation

A total of 2 μL of carboxylic acid-functionalized magnetic beads (Invitrogen, 14305D) were suspended in 100 μL of 0.01 M NaOH and rotated at room temperature for 10 min. Beads were washed by placing the tube on a magnet for 2 min, and the supernatant was removed. A total of 100 μL of deionized water was then added to the beads and the tube was hand tumbled, then washed with the magnet. 1-Ethyl-3-(3-dimethylaminopropyl)carbodiimide (EDC) solution (50 mg/mL EDC in cold deionized water) was added to the beads which were rotated for 30 min. Beads were washed on the magnet and resuspended in cold dH_2O , after which they were hand tumbled, placed on the magnet, and washed again. A total of 100 μL of 100 mM 2-(N-morpholino)ethanesulfonic acid (MES) was added, and the tube was hand tumbled and washed. Beads were resuspended in 100 μL of 100 mM MES with 33 pmol binding immunoglobulin protein GRP78 (Abcam, ab78432) for 30 min at room temperature then washed. A total of 500 μL of 0.05 M Tris (pH 7.4) was added to the tube which was then hand tumbled and washed. The contents were then washed with 500 μL PBS with 1 g/L bovine serum albumin (PBSA).

4.5 | Magnetic Activated Cell Sorting

Monovalent magnetic bead selections were performed generally as previously described (Ackerman et al. 2009). At least 10 \times library diversity of induced yeast was washed with 1 mL PBSA then mixed with 10 μL bare streptavidin Dynabeads (Thermo Fisher Scientific, 11205D) and incubated for 2 h at 4°C while rotating. Cells were placed on a magnet for 5 min, then unbound cells were transferred to a fresh tube and incubated with prepared binding immunoglobulin protein-coated carboxylic acid beads. The mixture was incubated for 2 h at 4°C while rotating. Cells were again placed on the magnet for 5 min, and unbound cells removed and added to a fresh tube. These cells were added to 25 nM biotinylated HEK293 cell lysate and incubated while rotating at 4°C for 1 h. After the hour, 10 μL bare streptavidin beads were added to the mixture and incubated for 2 h at 4°C while rotating. Cells were placed on the magnet for 5 min, then supernatant was removed, and the bead-bound cells were grown up in SD-CAA.

4.6 | Fluorescent Activated Cell Sorting

Fluorescent activated cell sorting generally followed previously established protocols (Chen et al. 2013). Induced yeast cultures were washed (8000g for 1 min) with 1 mL PBSA and then incubated with cell lysate and 17 nM anti cMyc antibody (Biolegend, 658502) for 2 h while rotating at 4°C. Cells were washed with 1 mL PBSA and fluorescently labeled with 17 nM anti-mouse AlexaFluor 647 (Invitrogen) for 20 min, rotating at 4°C. Cells were washed with 1 mL PBSA, and cells with the highest ratio of binding to displayed ligand (top 0.2% and next 2%) were collected via the FACS Aria II cell sorter (Becton, Dickinson and company) at the University of Minnesota Flow Cytometry Resource.

4.7 | On-Yeast Protease Assay

A total of 10⁷ induced yeast cells were washed (8000g for 1 min) with 1 mL PBSA and resuspended in 50 μL PBSA. Cells were

moved to a 200 μ L PCR tube and mixed with 50 μ L proteinase K (NEB, P8107S) to yield a final concentration of 1 U/L (proteinase K diluted in PBSA) and placed on ice. Cells were quickly transferred to a PCR block prechilled to 4°C and incubated for 10 min at 37°C (Eppendorf Mastercycler Nexus GX2). After incubation, cells were moved quickly to ice and transferred into 1 mL ice cold PBSA. Cells were centrifuged at 8000g for 1 min (rotor prechilled to 4°C).

HA and cMyc epitope tags were labeled with 17 nM chicken anti-HA (Abcam, ab9111) and 34 nM mouse anti-cMyc (Biolegend, 658502) for 30 min at room temperature with rotation. Cells were washed with 1 mL PBSA (8000g for 1 min) and incubated with 17 nM goat anti-chicken AlexaFluor647 (Invitrogen) and 34 nM FITC anti-mouse IgG for 20 min at 4°C with rotation (Biolegend, 406001). Cells were washed with 1 mL PBSA and sorted via FACS using BD FACSAria II (BD). Cells were collected in 4 gates based on cMyc to HA ratio (top 10%, next 20%, next 30%, and remaining 40%).

4.8 | Yeast Display Level Assay

Yeast cultures were grown up in SD-CAA to an OD₆₀₀ greater than 4 and then induced for 18 h at 37°C instead of the usual 30°C. The cMyc epitope tag was labeled in the same manner explained above and sorted based on FITC signal into 4 tiered gates as with the on-yeast protease assay.

4.9 | Multiplex Deep Sequencing

DNA plasmids encoding for the affibody proteins were extracted from yeast via zymoprep (Zymo Research) following manufacturer's instructions. A total of 5×10^7 – 10×10^7 yeast cells were spun down for 1 min at 8000g and the supernatant was removed. Cells were then resuspended in 200 μ L zymo solution 1, after which 2 μ L β -mercaptoethanol and 10 μ L long-life zymolyase (Zymo Research) was added. Cells were incubated statically for at least 3 h at 37°C and briefly vortexed every hour. After incubation, cells were frozen for 15 min in the –80°C freezer and then thawed. A total of 200 μ L of MX2 (Epoch) was added to the thawed tubes and mixed, and the tubes were allowed to sit for 3 min. A total of 400 μ L MX3 (Epoch) was then added, tubes briefly vortexed, and centrifuged at 16,000g for 8 min. Supernatant was added to an Epoch DNA column and centrifuged at 8000g for 1 min. After removing flowthrough, 750 μ L of WS (Epoch) was added to the tubes and allowed to sit for 3 min. The tubes were then centrifuged for 1 min at 8000g. After removing flowthrough, the tubes were centrifuged again for 1 min at 12,000g to remove any residual WS. Plasmid DNA was eluted by moving the filter column to a fresh tube and adding 32 μ L EB (Epoch), which was allowed to sit for 1 min before centrifuging at 12,000g for 1 min.

Plasmid DNA was first amplified with Q5 DNA polymerase (NEB) using the manufacturer's protocol to add universal overhangs to all sequences (primers indicated in Supporting Information S1: Table S3). Following this PCR, 2 μ L of exonuclease I was added, and tubes were incubated for 30 min at 37°C and 20 min at 80°C. The next PCR was done using the same protocol but with unique primers to add barcoded multiplex

deep sequencing adapters to each pool of DNA. PCR product was verified via 1% agarose gel, and bands were extracted using the GenCatch extraction kit (Epoch).

All multiplex deep sequencing was performed by the University of Minnesota Genomics Center utilizing MiSeq (Illumina). Using USEARCH software (Edgar 2010), raw reads were merged, denoised and filtered. Unique reads from each DNA pool were identified and counted. DNA sequences were then translated to amino acid sequences and output to a dataframe for further analysis. Data are available at <https://github.com/HackellLab-UMN>. Binding strength was assessed based on enrichment from the error-prone PCR library and the FACS sorted binding pool. Developability assay scores were calculated as the weighted average score (Equation 1, with α being the gate weight calculated as the midpoint of the bottom and top percentiles of the gate [e.g., 0.95, 0.8, 0.55, 0.2]).

$$\text{Score } (n \text{ occurrences of clone } i \text{ in gate } j) = \sum_1^{n_i} \frac{\alpha_j * n_{i,j}}{n_i}. \quad (1)$$

4.10 | Cloning Variants Into Expression System

Variants were identified for characterization based on positive binding enrichment and above average developability scores. Genes encoding selected variants were synthesized (eBlock, IDT; Supporting Information S1: Table S5) with overhangs matching the pET expression vector to allow for Gibson assembly, carried out according to manufacturer's protocols (NEB, E2621S). eBlock variants were cloned into T7 Express *E. coli* cells according to manufacturer's protocols (NEB, C2566). Colonies from transformation were plucked and grown in LB + kanamycin overnight at 37°C and 250 RPM. Proper sequences were validated via Sanger sequencing (Eurofins).

4.11 | Protein Production and Purification

Fresh 5 mL cultures were started the day before protein production in LB + kanamycin and grown at 37°C and 250 RPM. A portion of the overnight culture was added to fresh LB + kanamycin to yield 100 mL at OD₆₀₀ = 0.1. The cultures were incubated at 37°C and 250 RPM for approximately 2 h, or until OD₆₀₀ reached between 0.60 and 1.0. Cells were induced for 2–2.5 h at 37°C and 250 RPM by adding 100 μ L 0.5 M IPTG. After incubation, cultures were centrifuged at 3200g for 10 min, aspirated, and resuspended in 1 mL active lysis buffer (9.38 g sodium phosphate dibasic heptahydrate, 2.07 g sodium phosphate monobasic monohydrate, 29.2 g sodium chloride, 50 mL glycerol, 3.1 g 3-((3-cholamidopropyl)dimethylammonio)-1-propanesulfonate (CHAPS), 1.7 g imidazole, with volume adjusted to 1 L with water) with EDTA-free protease inhibitor pellet (ThermoFisher, A32955). Cells were frozen at –80°C and thawed 4 \times , then centrifuged (12,000g, 10 min, 4°C). Supernatant was passed through a 0.22 μ m filter and stored at 4°C briefly. Protein was purified using HisPur Cobalt resin (ThermoFisher, 89964). A total of 200 μ L cobalt resin was added to cell lysate and allowed to bind for at least 10 min. The mixture was washed with 750 μ L of 30 mM imidazole in PBS 5 times and washed once with 750 μ L 50 mM imidazole in PBS. Protein was eluted with 350 μ L 300 mM imidazole in PBS. Purified

protein was buffer-exchanged into 1× PBS to remove imidazole using Slide-A-Lyzer MINI Dialysis 5 K MWCO (ThermoFisher). Dialysis units were placed into 1000× volume PBS and incubated for 3 h with fresh PBS added every hour. After the final round of fresh PBS addition, the units were left stirring at 4°C for 24 h to complete the buffer exchange.

4.12 | Protein Electrophoresis

A total of 12 µL of purified protein was combined with 4 µL lithium dodecyl sulfate buffer and 0.5 µL β-mercaptoethanol and heated to 95°C for 10 min to denature protein. Lysozyme standard was included at 4 different concentrations to assess affibody concentration. Samples and PageRuler prestained ladder (ThermoFisher) were loaded onto a NuPAGE Bis-Tris gel (Invitrogen). Gels were electrophoresed for 30 min at 185 V, then washed and stained with SimplyBlue SafeStain (Invitrogen). ImageJ was used to quantify band intensity and calculate protein yield using a calibration curve from the lysozyme standards.

4.13 | Affinity Titrations

HEK293 cells expressing either TNFR1 or DR5 were incubated with varying concentrations of His₆-tagged affibody proteins at 4°C. The affibody/receptor ratio was held constant in all cases and all tubes were incubated for the same time, based on the shortest duration required to ensure a minimum of 90% equilibrium binding for the lowest concentration condition (assuming k_{on} of $2.5 \times 10^5 \text{ M}^{-1}\text{s}^{-1}$). Cells were then washed with 1 mL PBSA (200g for 2 min) and incubated with anti-His₆ APC antibody (Biolegend, 362605), rotating for 20 min at 4°C. Binding was measured using the BD Accuri C6 and quantified as the median APC signal for each condition. K_D was calculated using GraphPad Prism via a global fit with normalization of all data points to the B_{max} of the fit binding curve.

4.14 | Circular Dichroism

A minimum of 0.1 mg/mL purified protein was loaded into the Picoland Jasco J815 circular dichroism spectropolarimeter. Molar ellipticity was monitored at 216 nm as temperature was ramped from 25°C to 95°C, sampling every 1°C with a ramp rate of 3°C/min. The midpoint of thermal denaturation was calculated from a standard two state unfolding curve.

Author Contributions

Study guidance: Benjamin J. Hackel and Jonathan N. Sachs. study design: Gregory H. Nielsen and Benjamin J. Hackel. Experimental work: Gregory H. Nielsen. data analysis: Gregory H. Nielsen and Benjamin J. Hackel. manuscript writing: Gregory H. Nielsen, Benjamin J. Hackel, and Jonathan N. Sachs.

Acknowledgments

We appreciate assistance from the University of Minnesota Flow Cytometry Resource as well as the University of Minnesota Genomics Center. This work was supported by the National Institutes of Health (R01 EB028274 and R01 GM146372).

Conflicts of Interest

The authors declare no conflicts of interest.

Data Availability Statement

The data that support the findings of this study are openly available in GitHub at <https://github.com/HackelLab-UMN>.

References

- Abramson, J., J. Adler, J. Dunger, et al. 2024. "Accurate Structure Prediction of Biomolecular Interactions With AlphaFold 3." *Nature* 630: 493–500.
- Ackerman, M., D. Levary, G. Tobon, B. Hackel, K. D. Orcutt, and K. D. Wittrup. 2009. "Highly Avid Magnetic Bead Capture: An Efficient Selection Method for De Novo Protein Engineering Utilizing Yeast Surface Display." *Biotechnology Progress* 25: 774–783.
- Van Antwerp, J. J., and K. D. Wittrup. 2000. "Fine Affinity Discrimination by Yeast Surface Display and Flow Cytometry." *Biotechnology Progress* 16: 31–37.
- Cazanave, S. C., J. L. Mott, S. F. Bronk, et al. 2011. "Death Receptor 5 Signaling Promotes Hepatocyte Lipoapoptosis." *Journal of Biological Chemistry* 286: 39336–39348.
- Chen, T. F., S. de Picciotto, B. J. Hackel, and K. D. Wittrup. 2013. "Engineering Fibronectin-Based Binding Proteins by Yeast Surface Display." *Methods in Enzymology* 523: 303–326.
- Chen, Z., X. Wang, X. Chen, et al. 2023. "Accelerating Therapeutic Protein Design With Computational Approaches Toward the Clinical Stage." *Computational and Structural Biotechnology Journal* 21: 2909–2926.
- Cortese, R., L. Prosperini, A. Stasolla, et al. 2021. "Clinical Course of Central Nervous System Demyelinating Neurological Adverse Events Associated With Anti-TNF Therapy." *Journal of Neurology* 268: 2895–2899.
- DeLano, W. L. 2002. "PyMol an Open-Source Molecular Graphics Tool." In *CCP4 Newsletter on Protein Crystallography*: 44–53.
- Drummond, D. A., B. L. Iverson, G. Georgiou, and F. H. Arnold. 2005. "Why High-Error-Rate Random Mutagenesis Libraries Are Enriched in Functional and Improved Proteins." *Journal of Molecular Biology* 350: 806–816.
- Edgar, R. C. 2010. "Search and Clustering Orders of Magnitude Faster Than BLAST." *Bioinformatics* 26: 2460–2461.
- Fernández-Quintero, M. L., A. Ljungars, F. Waibl, et al. 2023. "Assessing Developability Early in the Discovery Process for Novel Biologics." *mAbs* 15: 2171248.
- Fischer, R., R. E. Kontermann, and K. Pfizenmaier. 2020. "Selective Targeting of TNF Receptors as a Novel Therapeutic Approach." *Frontiers in Cell and Developmental Biology* 8: 401.
- Golinski, A. W., K. M. Mischler, S. Laxminarayan, et al. 2021. "High-Throughput Developability Assays Enable Library-Scale Identification of Producing Protein Scaffold Variants." *Proceedings of the National Academy of Sciences* 118: e2026658118.
- Golinski, A. W., Z. D. Schmitz, G. H. Nielsen, et al. 2023. "Predicting and Interpreting Protein Developability via Transfer of Convolutional Sequence Representation." *ACS Synthetic Biology* 12: 2600–2615.
- B. Hackel. 2009. "Fibronectin Domain Engineering." Doctoral Dissertation, MIT.
- Hackel, B. J., M. E. Ackerman, S. W. Howland, and K. D. Wittrup. 2010. "Stability and CDR Composition Biases Enrich Binder Functionality Landscapes." *Journal of Molecular Biology* 401: 84–96.
- Hackel, B. J., A. Kapila, and K. Dane Wittrup. 2008. "Picomolar Affinity Fibronectin Domains Engineered Utilizing Loop Length Diversity, Recursive Mutagenesis, and Loop Shuffling." *Journal of Molecular Biology* 381: 1238–1252.

- Hirsova, P., and G. J. Gores. 2015. "Death Receptor-Mediated Cell Death and Proinflammatory Signaling in Nonalcoholic Steatohepatitis." *Cellular and Molecular Gastroenterology and Hepatology* 1: 17–27.
- Hirsova, P., S. H. Ibrahim, G. J. Gores, and H. Malhi. 2016. "Lipotoxic Lethal and Sublethal Stress Signaling in Hepatocytes: Relevance to NASH Pathogenesis." *Journal of Lipid Research* 57: 1758–1770.
- Jain, T., T. Boland, and M. Vásquez. 2023. "Identifying Developability Risks for Clinical Progression of Antibodies Using High-Throughput In Vitro and In Silico Approaches." *mAbs* 15: 2200540.
- Jain, T., T. Sun, S. Durand, et al. 2017. "Biophysical Properties of the Clinical-Stage Antibody Landscape." *Proceedings of the National Academy of Sciences* 114: 201616408.
- Jones, D. S., P.-C. Tsai, and J. R. Cochran. 2011. "Engineering Hepatocyte Growth Factor Fragments With High Stability and Activity as Met Receptor Agonists and Antagonists." *Proceedings of the National Academy of Sciences* 108: 13035–13040.
- Kelly, R. L., J. C. Geoghegan, J. Feldman, et al. 2017. "Chaperone Proteins as Single Component Reagents to Assess Antibody Non-specificity." *mAbs* 9: 1036–1040.
- Klesmith, J. R., L. Su, L. Wu, et al. 2019. "Retargeting CD19 Chimeric Antigen Receptor T Cells via Engineered CD19-Fusion Proteins." *Molecular Pharmaceutics* 16: 3544–3558.
- Löfblom, J., J. Feldwisch, V. Tolmachev, J. Carlsson, S. Ståhl, and F. Y. Frejd. 2010. "Affibody Molecules: Engineered Proteins for Therapeutic, Diagnostic and Biotechnological Applications." *FEBS Letters* 584: 2670–2680.
- Lown, P. S., J. J. Cai, S. C. Ritter, J. J. Otolski, R. Wong, and B. J. Hackel. 2021. "Extended Yeast Surface Display Linkers Enhance the Enrichment of Ligands in Direct Mammalian Cell Selections." *Protein Engineering, Design & Selection: PEDS* 34: 1–9.
- Nielsen, G. H., Z. D. Schmitz, and B. J. Hackel. 2024. "Sequence-Developability Mapping of Affibody and Fibronectin Paratopes via Library-Scale Variant Characterization." *Protein Engineering, Design and Selection* 37: gzae010.
- Nord, K., E. Gunneriusson, J. Ringdahl, S. Ståhl, M. Uhlén, and P. Å. Nygren. 1997. "Binding Proteins Selected From Combinatorial Libraries of an α -Helical Bacterial Receptor Domain." *Nature Biotechnology* 15: 772–777.
- Probert, L. 2015. "TNF and Its Receptors in the CNS: The Essential, the Desirable and the Deleterious Effects." *Neuroscience* 302: 2–22.
- Ritter, S. C., and B. J. Hackel. 2019. "Validation and Stabilization of a Prophage Lysin of *Clostridium Perfringens* by Using Yeast Surface Display and Coevolutionary Models." *Applied and Environmental Microbiology* 85: e00054-19.
- Rocklin, G. J., T. M. Chidyausiku, I. Goreschnik, et al. 2017. "Global Analysis of Protein Folding Using Massively Parallel Design, Synthesis, and Testing." *Science* 357: 168–175.
- Shakoor, N., M. Michalska, C. A. Harris, and J. A. Block. 2002. "Drug-Induced Systemic Lupus Erythematosus Associated With Etanercept Therapy." *Lancet* 359: 579–580.
- Shusta, E. V., P. D. Holler, M. C. Kieke, D. M. Kranz, and K. D. Wittrup. 2000. "Directed Evolution of a Stable Scaffold for T-Cell Receptor Engineering." *Nature Biotechnology* 18: 754–759.
- Shusta, E. V., M. C. Kieke, E. Parke, D. M. Kranz, and K. D. Wittrup. 1999. "Yeast Polypeptide Fusion Surface Display Levels Predict Thermal Stability and Soluble Secretion Efficiency." *Journal of Molecular Biology* 292: 949–956.
- Tokuriki, N., F. Stricher, L. Serrano, and D. S. Tawfik. 2008. "How Protein Stability and New Functions Trade Off." *PLoS Computational Biology* 4: e1000002.
- Tokuriki, N., and D. S. Tawfik. 2009. "Protein Dynamism and Evolvability." *Science* 324: 203–207.
- Vunnam, N., M. Been, E. Huber, et al. 2023. "Discovery of a Non-Competitive TNFR1 Antagonist Affibody With Picomolar Monovalent Potency That Does Not Affect TNFR2 Function." *Molecular Pharmaceutics* 20: 1884–1897.
- Vunnam, N., S. Szymonski, P. Hirsova, G. J. Gores, J. N. Sachs, and B. J. Hackel. 2020. "Noncompetitive Allosteric Antagonism of Death Receptor 5 by a Synthetic Affibody Ligand." *Biochemistry* 59: 3856–3868.
- Woldring, D. R., P. V. Holec, H. Zhou, and B. J. Hackel. 2015. "High-Throughput Ligand Discovery Reveals a Sitewise Gradient of Diversity in Broadly Evolved Hydrophilic Fibronectin Domains." *PLoS One* 10: e0138956.
- Wolf Pérez, A. M., P. Sormanni, J. S. Andersen, et al. 2019. "In Vitro and In Silico Assessment of the Developability of a Designed Monoclonal Antibody Library." *mAbs* 11: 388–400.
- Wolfe, F., and K. Michaud. 2004. "Lymphoma in Rheumatoid Arthritis: The Effect of Methotrexate and Anti-Tumor Necrosis Factor Therapy in 18,572 Patients." *Arthritis & Rheumatism* 50: 1740–1751.
- Yeung, Y. A., and K. D. Wittrup. 2002. "Quantitative Screening of Yeast Surface-Displayed Polypeptide Libraries by Magnetic Bead Capture." *Biotechnology Progress* 18: 212–220.
- Zaccolo, M., D. M. Williams, D. M. Brown, and E. Gherardi. 1996. "An Approach to Random Mutagenesis of DNA Using Mixtures of Triphosphate Derivatives of Nucleoside Analogues." *Journal of Molecular Biology* 255: 589–603.

Supporting Information

Additional supporting information can be found online in the Supporting Information section.